FORCED CONVECTION OF RADIATING GAS OVER AN INCLINED BACKWARD FACING STEP USING THE BLOCKED-OFF METHOD

by

Amir Babak ANSARI * **and Seyyed Abdolreza GANDJALIKHAN NASSAB**

Mechanical Engineering Department, School of Engineering, Shahid Bahonar University, Kerman, Iran

Original scientific paper
DOI: 10.2298/TSCI110112132A

The present work investigates the laminar forced convection flow of a radiating gas over an inclined backward facing step in a horizontal duct. The momentum and energy equations are solved numerically by the computational fluid dynamics techniques to obtain the velocity and temperature fields. Since, the 2-D Cartesian co-ordinate system is used to solve the governing equations; the flow over inclined surface is simulated by considering the blocked-off region in regular grid. Discretized forms of the governing equations in the (x,y) plane are obtained by the control volume method and solved using the SIMPLE algorithm. The fluid is treated as a gray, absorbing, emitting, and scattering medium. Therefore, all of the convection, conduction and radiation heat transfer mechanisms take place simultaneously in the gas flow. For computation of the radiative term in the gas energy equation, the radiative transfer equation is solved numerically by the discrete ordinates method to find the radiative heat flux distribution inside the radiating medium. In the numerical results, effects of inclination angle, optical thickness, scattering albedo and the radiation-conduction parameter on the heat transfer behavior of the convection flow are investigated. This research work is a new one in which a combined convection-radiation thermal system with a complex flow geometry is simulate by efficient numerical techniques.

Key words: *backward facing step, laminar forced convection flow, radiation heat transfer, blocked-off method*

Introduction

Forced convection flow in channels with abrupt contraction or expansion in flow geometry is widely encountered in engineering applications. In many cases such as flow over gas turbine blades and the combustion product, the radiation heat transfer may be important. Also the trend toward increasing temperature in modern technological systems has promoted concerted effort to develop more comprehensive and accurate theoretical methods to treat radiation. Therefore, for having more accurate and reliable results in the analysis, the gas flow must be considered as a radiating medium and all of the heat transfer mechanisms including convection, conduction and radiation, must be taken into account. The flow over backward facing step (BFS) has the most features of separated flows. Although, the geometry of BFS flow is very simple, but the heat transfer and fluid flow over this type of step contain most of complexities. Consequently, it has been used in the benchmark investigations.

There are many studies about laminar convection flow over BFS in a duct by several investigators. Armaly *et al.* [1, 2] studied laminar, transition, and turbulent isothermal flow over

* Corresponding author; e-mail: aba2449@yahoo.com

a BFS, experimentally and theoretically. Erturk [3] investigated the characteristics of the flow over a 2-D BFS in a wide range of Reynolds number. Abu-Nada [4-6] analyzed the convection flow over BSF step in a duct to investigate the amount of entropy generation in this type of flow. In that work, the set of governing equations were solved by the finite volume method, and the distributions of entropy generation number, friction coefficient and Nusselt number on the duct walls were calculated. Moreover, the effect of suction and blowing on the entropy generation number and Bejan number were presented. A review of research on laminar convection flow over backward and forward facing step was done by Abu-Mulaweh [7]. In that study, a comprehensive review of such flows, those have been reported in several studies in the open literature was presented. The purpose was to give a detailed summery of the effect of several parameters such as step height, Reynolds and Prandtl number and the buoyancy force on the flow and temperature distributions downstream of the step. Several correlation equations reported in many studies were also summarized in that review.

In all of the above works, the step was considered to be vertical to the bottom wall. It is obvious that there are many engineering applications, in which the forward- or backward-facing step is inclined. In a recent study, Gandjalikhan Nassab *et al.* [8] studied the turbulent forced convection flow adjacent to inclined forward step in a duct. In that study, the Navier-Stokes and energy equations were solved in the computational domain by computational fluid dynamics (CFD) method using conformal mapping technique. By this method, the effect of step inclination angle on flow and temperature distributions was determined.

Thermal radiation coupled with forced convection is an important issue for engineering applications, such as heat exchangers and combustion chambers. When the flowing gas behaves as a participating medium, its complex absorption, emission and scattering introduce a considerable difficulty in the simulation of these flows. In all of the research studies mentioned above, the effect of radiation heat transfer is neglected in the analysis, such that the gas energy equation only contains the convection and conduction terms. There are limited numbers of literatures available dealing with the radiative transfer problems with complex 2-D and 3-D geometries. In a literature overview on coupled heat transfer in high temperature radiating gas flows, an effective model was employed by Viskanta [9] for analyzing the combined radiative-convective thermal systems. Azad and Modest [10] investigated the problem of combined radiation and turbulent forced convection in absorbing, emitting and linearly anisotropic scattering gas particulate flow through a circular tube. Bouali and Mearhab [11] studied heat transfer by laminar forced convection and surface radiation in a divided vertical channel with isotherm side walls. They found that the surface radiation has important effect on the Nu at high Re. Barhaghi and Davidson [12] studied a mixed convection-radiation heat transfer in a vertical channel, using large eddy simulation. Two different cases for the Grashof number of to Re number ratios based on the wall heat flux and the channel width, were considered by applying constant heat flux boundary condition to one of the channel walls while the other wall was kept insulated. Also, the radiation heat transfer was assumed to be 2-D, and the span-wise variation of the radiation was neglected. It was found that the fluid property variation has a considerable effect on the temperature distribution.

As the convection flow over backward facing inclined step has many applications in engineering, the present work deals the analysis of this type of flow, in which all of the heat transfer mechanisms including convection, conduction, and radiation take place simultaneously in the fluid flow. For this purpose, the set of governing equations are solved by the CFD technique in the Cartesian co-ordinate system using the blocked-off method, while in calculation of radiative heat flux distribution inside the participating medium, the well known discrete ordinates method is employed. It should be noted that the analysis of convection flow over inclined BFS with considering the gas radiation effect is done in the present work for the first time, with using the well known blocked-off technique.

Theory

2-D laminar force convection of steady air flow, in a 2-D horizontal heated rectangular duct over an inclined BFS and with considering the gas radiation effect is numerically simulated. Schematic of the computational domain is shown in fig. 1. The upstream and downstream heights of the duct are *h* and *H*, respectively, such that this geometry provides a BFS height of *s*, with an expansion ratio of $ER = H/h$, which is considered equal to 2 in the present computations. The upstream length of the duct is considered to be $L_1 = 2H$ and the downstream length of the duct is $L_2 = 20H$. This is made to ensure that the flow at the inlet section of the duct ($X = -2$) is not affected significantly by the sudden expansion in the geometry at the step and the flow at the exit section ($X = 20$) becomes fully developed. The step is considered to be inclined with inclination angle of ϕ which is evaluated from the horizontal co- -ordinate.

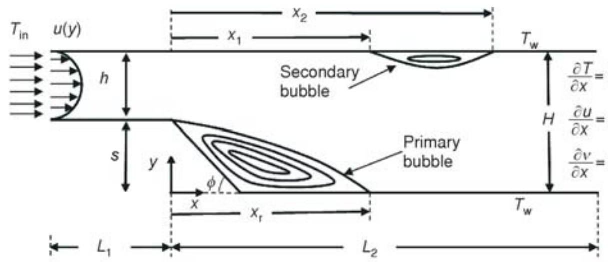

Figure 1. Sketch of problem geometry

The boundary conditions are treated as no slip conditions at the solid walls (zero velocity) and constant temperature of T_w at the bottom and top walls. At the inlet duct section, the flow is fully developed with uniform temperature of T_{in}, which is assumed to be lower than T_w. At the outlet section, zero axial gradients for velocity components and gas temperature are employed.

Basic equations

For incompressible, steady and 2-D laminar convection flow, the governing equations are the conservations of mass, momentum, and energy equation that can be written as follows:

$$\frac{\partial u}{\partial x} + \frac{\partial v}{\partial y} = 0 \tag{1}$$

$$u\frac{\partial u}{\partial x} + v\frac{\partial u}{\partial y} = -\frac{1}{\rho}\frac{\partial p}{\partial x} + \frac{\mu}{\rho}\left(\frac{\partial^2 u}{\partial x^2} + \frac{\partial^2 u}{\partial y^2}\right) \tag{2}$$

$$u\frac{\partial v}{\partial x} + v\frac{\partial v}{\partial y} = -\frac{1}{\rho}\frac{\partial p}{\partial y} + \frac{\mu}{\rho}\left(\frac{\partial^2 v}{\partial x^2} + \frac{\partial^2 v}{\partial y^2}\right) \tag{3}$$

$$\frac{\partial}{\partial x}(\rho u c_p T) + \frac{\partial}{\partial y}(\rho v c_p T) = k\left(\frac{\partial^2 T}{\partial x^2} + \frac{\partial^2 T}{\partial y^2}\right) - \nabla \vec{q}_r \tag{4}$$

Gas radiation modeling

Since, gas radiation effect is considered in the simulation, besides the convective and conductive terms, the radiative term also presents in the energy equation. In this equation, $\nabla \vec{q}_r$ can be calculated as [13]:

$$\nabla \vec{q}_r = \sigma_a [4\pi I_b(\vec{r}) - \int_{4\pi} I(\vec{r},\vec{s}) d\Omega] \tag{5}$$

where, σ_a is the absorption coefficient, $I(\vec{r},\vec{s})$ – the radiation intensity at position $\vec{r}$ and in the direction $\vec{s}$ and $I_b(\vec{r}) = \sigma[T(\vec{r})]^4/\pi$ – the black body radiation intensity. To obtain the radiation intensity field and $\nabla \vec{q}_r$, it is necessary to solve the radiative transfer equation (RTE). This equation for an absorbing, emitting and scattering gray medium can be written as [13]:

$$(\vec{s}\nabla) I(\vec{r},\vec{s}) = -\beta I(\vec{r},\vec{s}) + \sigma_a I_b(\vec{r}) + \frac{\sigma_s}{4\pi} \int_{4\pi} I(\vec{r},\vec{s}) \varphi(\vec{s},\vec{s}\,') d\Omega' \tag{6}$$

in which σ_s is the scattering coefficient, σ_a – the absorption coefficient, $\beta = \sigma_a + \sigma_s$ – the extinction coefficient, and $\varphi(\vec{s},\vec{s}\,')$ – the scattering phase function for the radiation from incoming direction $\vec{s}\,'$ and confined within the solid angle $d\Omega'$ to scattered direction $\vec{s}$ confined within the solid angle $d\Omega$. In this study, isotropic scattering medium is considered, in which the phase function is equal to unity. The boundary condition for a diffusely emitting and reflecting gray wall is:

$$I(\vec{r}_w,\vec{s}) = \varepsilon_w I_b(\vec{r}_w) + \frac{1-\varepsilon_w}{\pi} \int_{\vec{n}_w,\vec{s}\,'<0} I(\vec{r}_w,\vec{s}) |\vec{n}_w,\vec{s}\,'| d\Omega' \quad \vec{n}_w,\vec{s} > 0 \tag{7}$$

where ε_w is the wall emissivity, $I_b(\vec{r}_w)$ – the black body radiation intensity at the temperature of the boundary surface, and $\vec{n}_w$ – the outward unit vector normal to the surface. Since, the RTE depends on the temperature field through the emission term, $I_b(\vec{r}_w)$, thus it must be solved simultaneously with overall energy equation. Here the discrete ordinates method (DOM) is used to solve the RTE.

In the DOM, eq. (6) is solved for a set of n different directions, $\vec{s}_i$, $i = 1, 2, 3,\dots,n$ and integrals over solid angle are replaced by the numerical quadrature, that is:

$$\int_{4\pi} f(\vec{s}) d\Omega \cong \sum_{i=1}^{n} w_i f(\vec{s}_i) \tag{8}$$

where w_i are the quadrature weights associated with the directions $\vec{s}_i$. By this method, eq. (6), is approximated by a set of n different equations, as follows:

$$(\vec{s}_i\nabla) I(\vec{r},\vec{s}_i) = -\beta I(\vec{r},\vec{s}_i) + \sigma_a I_b(\vec{r}) + \frac{\sigma_s}{4\pi} \sum_{j=1}^{n} I(\vec{r},\vec{s}_j) \varphi(\vec{s}_j,\vec{s}_i) w_i \quad i = 1, 2, 3,\dots,n \tag{9}$$

subjected to the boundary conditions:

$$I(\vec{r}_w,\vec{s}_i) = \varepsilon_w I_b(\vec{r}_w) + \frac{1-\varepsilon_w}{\pi} \sum_{\vec{n}_w,\vec{s}_j<0} I(\vec{r}_w,\vec{s}_j) |\vec{n}_w,\vec{s}_j| w_j \quad \vec{n}_w,\vec{s}_i > 0 \tag{10}$$

and the divergence of the radiative heat flux is expressed as:

$$\nabla \vec{q}_r = \sigma_a [4\pi I_b(\vec{r}) - \sum_{i=1}^{n} I(\vec{r},\vec{s}_i) w_i] \tag{11}$$

At a surface, heat flux may also be determined from surface energy balance as:

$$\vec{q}\vec{n}(\vec{r}_w) \cong \varepsilon_w [\pi I_b(\vec{r}_w) - \sum_{\vec{n},\vec{s}_i<0} w_i I_i(\vec{r}_w) |\vec{n},\vec{s}_i|] \tag{12}$$

In 2-D Cartesian co-ordinate system, eq. (9) becomes:

$$\xi_i \frac{\partial I_i}{\partial x} + \eta_i \frac{\partial I_i}{\partial y} + \beta I_i = \beta S_i \quad i = 1,2,3,\dots,n \tag{13}$$

where S_i is a shorthand for the radiative source function that can be calculated by the following equation:

$$S_{\mathrm{i}} = (1-\omega) I_{\mathrm{b}}(\vec{\mathrm{r}}) + \frac{\omega}{4\pi} \sum_{j=1}^{n} I(\vec{\mathrm{r}}, \vec{\mathrm{s}}_{\mathrm{j}}) \varphi(\vec{\mathrm{s}}_{\mathrm{j}}, \vec{\mathrm{s}}_{\mathrm{i}}) w_{\mathrm{j}} \quad i = 1, 2, 3, \ldots, n \tag{14}$$

in which ω is the scattering albedo. The finite volume form of eq. (13) gives the following form for radiant intensity [13]:

$$I_{pi} = \frac{|\xi_i| A_x I_{xi} + |\eta_i| A_y I_{yi} + \beta \forall S_{pi}}{\beta \forall + |\xi_i| A_x + |\eta_i| A_y} \tag{15}$$

in which ξ_{i} and η_{i} are the direction cosines for the direction $\vec{\mathrm{s}}_{\mathrm{i}}$ and $\forall$ is the element cell volume. The details of the numerical solution of RTE by the DOM were also described in [14], in which the thermal characteristics of porous radiant burners were investigated.

For the radiative boundary conditions, the walls are assumed to emit and reflect diffusely with constant wall emissivity, $\varepsilon_{\mathrm{w}} = 0.8$. In addition, the inlet and outlet sections are considered as black walls at the temperature of inlet and outlet sections, respectively.

In the convection flow of a radiating gas, the energy transport from the duct wall to the gas flow depends on two related factors, the fluid temperature gradient on the wall and the rate of radiative heat exchange. Therefore, the local total Nusselt number along the duct walls is defined as $\mathrm{Nu}_{\mathrm{t}} = q_{\mathrm{t}} D_{\mathrm{h}}/k(T_{\mathrm{w}} - T_{\mathrm{b}})$ where $q_{\mathrm{t}} = q_{\mathrm{c}} + q_{\mathrm{r}} = -k\partial T/\partial y + q_{\mathrm{r}}$ and D_{h} is the hydraulic diameter which is equal to 2 h. The function Nu_{t} is the sum of local convective Nu number, Nu_{c}, and local radiative Nusselt number, Nu_{r}.

Non-dimensional forms of the governing equations

In numerical solution of the set of governing equations including the continuity, momentum and energy, the following dimensionless parameters are used to obtain the non-dimensional forms of these equations:

$$(X,Y) = \left(\frac{x}{D_{\mathrm{h}}}, \frac{y}{D_{\mathrm{h}}}\right), \quad (U,V) = \left(\frac{u}{U_{\mathrm{o}}}, \frac{v}{U_{\mathrm{o}}}\right), \quad P = \frac{p}{\rho U_o^2}, \quad I^* = \frac{I}{\sigma T_w^4}, \quad S^* = \frac{S}{\sigma T_w^4},$$
$$\vec{\mathrm{q}}_{\mathrm{r}}^* = \frac{\vec{\mathrm{q}}_{\mathrm{r}}}{\sigma T_w^4}, \quad \tau = \beta D_h, \quad (1-\omega) = \frac{\sigma_{\mathrm{a}}}{\beta}, \quad \Theta = \frac{T - T_{\mathrm{in}}}{T_{\mathrm{w}} - T_{\mathrm{in}}}, \quad \theta_1 = \frac{T_{\mathrm{in}}}{T_{\mathrm{w}} - T_{\mathrm{in}}}, \tag{16}$$
$$\theta_2 = \frac{T_{\mathrm{w}}}{T_{\mathrm{in}}}, \quad \mathrm{Pr} = \frac{\nu}{\alpha}, \quad \mathrm{Re} = \frac{\rho U_o D_h}{\mu}, \quad \mathrm{Pe} = \mathrm{Re\,Pr}, \quad RC = \frac{\sigma T_w^3 D_{\mathrm{h}}}{k}$$

The non-dimensional forms of the governing equations are:

$$\frac{\partial U}{\partial X} + \frac{\partial V}{\partial Y} = 0 \tag{17}$$

$$\frac{\partial}{\partial X}\left(U^2 - \frac{1}{\mathrm{Re}}\frac{\partial U}{\partial X}\right) + \frac{\partial}{\partial Y}\left(UV - \frac{1}{\mathrm{Re}}\frac{\partial U}{\partial Y}\right) = -\frac{\partial P}{\partial X} \tag{18}$$

$$\frac{\partial}{\partial X}\left(UV - \frac{1}{\mathrm{Re}}\frac{\partial V}{\partial X}\right) + \frac{\partial}{\partial Y}\left(V^2 - \frac{1}{\mathrm{Re}}\frac{\partial V}{\partial Y}\right) = -\frac{\partial P}{\partial Y} \tag{19}$$

$$\frac{\partial}{\partial X}\left(U\Theta - \frac{1}{\mathrm{Pe}}\frac{\partial \Theta}{\partial X}\right) + \frac{\partial}{\partial Y}\left(V\Theta - \frac{1}{\mathrm{Pe}}\frac{\partial \Theta}{\partial Y}\right) +$$
$$+ \frac{\tau(1-\omega) RC\,\theta_1 \theta_2}{\mathrm{Pe}}\left[\frac{4}{\theta_2^4}\left(\frac{\Theta}{\theta_1} + 1\right)^4 - \sum_{i=1}^{n} I_i^* w_i\right] = 0 \tag{20}$$

It should be noted that due to the small value of fluid velocity and Eckert number in the duct flow, the viscous dissipation term in the energy equation is omitted. The physical quantities of interest in heat transfer study are the mean bulk temperature and the Nu which are defined by:

$$\theta_{\mathrm{b}} = \frac{\int_0^1 \Theta U \mathrm{d}Y}{\int_0^1 U \mathrm{d}Y} \tag{21}$$

$$\mathrm{Nu}_{\mathrm{t}} = \mathrm{Nu}_{\mathrm{c}} + \mathrm{Nu}_{\mathrm{r}} = \frac{-1}{\Theta_{\mathrm{w}} - \Theta_{\mathrm{b}}} \left.\frac{\partial \Theta}{\partial Y}\right|_{Y=0} + \frac{RC\,\theta_1 \theta_2}{\Theta_{\mathrm{w}} - \Theta_{\mathrm{b}}} \vec{\mathrm{q}}_{\mathrm{r}}^{*} \tag{22}$$

Numerical procedure

In numerical solution of the Navier-Stokes and energy equations, eqs. (17) to (20), discretized forms of these equations were obtained by integrating over an element cell volume. The staggered type of control volume for the *x*- and *y*-velocity components was used, while the other variables of interest were computed at the grid nodes. Discretized forms of the governing equations were numerically solved by the SIMPLE algorithm of Patankar and Spalding [15]. Numerical solutions were obtained iteratively by the line-by-line method. Numerical calculations were performed by writing a computer program in FORTRAN. As the result of grid tests for obtaining the grid-independent solutions, extensive mesh testing was performed in tab. 1, in which the Nu on the bottom wall of the duct at the outlet section is calculated. The grid is concentrated close to the duct walls and near to the step corners, in order to ensure the accuracy of the numerical solution (fig. 2). As it is shown in tab. 1, a grid size of 600 × 50 can be chosen for obtaining the grid independent solution, such that the subsequent numerical calculations are made based on this grid size.

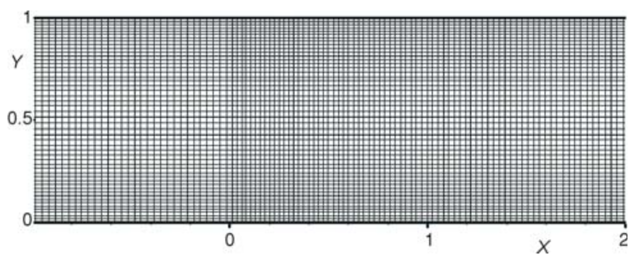

Figure 2. The schematic of grid generation

Table 1. Grid independence study, Re = 100, *RC* =150, τ = 0.005, ε = 0.8, ω = 0.5

Grid	300 × 20	400 × 30	500 × 40	600 × 50	650 × 60
$\mathrm{Nu_t}$	5.7526	5.9107	6.3766	6.4613	6.4628

Also, in solving the set of governing equations with a computer code written in FORTRAN, the calculation times for the above mesh sized are given in tab. 2. It should be mentioned that the following computer is used for computations: Intel(R), Pentium(R) 4, CPU 2.80 GHz and 512 MB of RAM.

Table 2. Time of calculation, Re = 100, RC = 150, τ = 0.005, ε = 0.8, ω = 0.5

Grid	300 × 20	400 × 30	500 × 40	600 × 50	650 × 60
Time [s]	84.6	288.7	686.2	1680.4	2345.1

In the computation of radiant intensity, the numerical solution of eq. (13), can be started with the black body assumption for the boundaries with neglecting the source term S_i. In the next iteration, the general forms of eq. (15) and its boundary condition are applied. This procedure is repeated until the convergence criterion is met for the distribution of radiant intensity. Finally, from the radiative intensity obtained by eq. (15), the divergence of radiative heat flux which is needed for the numerical solution of the energy equation can be calculated. Since, in the DOM, different numbers of discrete directions can be chosen during S_N approximation, the results obtained by the S_4, S_6, and S_8 approximations were compared and there was a small difference, less than 1% error, between S_4 and S_6 approximations. Therefore, S_4 approximation has been used in subsequent calculations. For calculating radiant intensity, the standard diamond difference scheme which is commonly used and has a good accuracy, is unstable and gives oscillatory and negative intensity solutions, especially when there is a significant difference between the radiation intensities on adjacent faces of the control volume. Therefore, the step scheme which is simple, convenient, stable and ensures positive intensities is employed.

Outline of strategy

The sequence of calculations can be summarized as follows:

(1) A first approximation for the variables u, v, p, and T at each node point is assumed.
(2) From the momentum equations in the x- and y-directions, the u- and v-velocity components are calculated.
(3) Pressure is calculated according to the SIMPLE algorithm.
(4) The RTE is solved for computing the distribution of the radiant intensity. Then the radiative source term in the energy equation is computed at each nodal point.
(5) From the energy equation, the temperature field is calculated inside the radiating medium.
(6) Steps 2-5 are repeated until convergence is obtained. This condition was assumed to have been achieved when the values of residual terms in the momentum and energy equations did not exceed 10^{-4}, with these criteria that in the numerical solution of RTE, the maximum difference between the radiative intensities computed during two consecutive iteration levels did not exceed 10^{-6} at each nodal point.

Blocked-off method

In order to avoid the complexity of treating non-orthogonal grids, it is suitable to formulate a procedure to model irregular geometries using Cartesian co-ordinates formulation. The blocked-off method consists on drawing nominal domains around given physical domain, so the whole 2-D region is divided into two parts: active and inactive or blocked-off regions. The control volumes which are inside the active region are designated as one (1) and otherwise they are zero (0), as shown in fig. 3. The region where solutions are sought is known as the active region and the remaining portion is known as the inactive or the blocked-off region. By this technique, the surface of inclined step in the present analysis is approximated by a series of rectangular steps. It is obvious that using fine grids in the interface region between active and inactive zones causes to have an approximated boundary which is more similar to the true boundary. For every type of geometry, a domain file has to be created. By changing the value of a control volume from 1 to 0, it can be made inactive. This domain file has to be created as per as the grid file for a particular problem.

According to the blocked-off technique, known values of the dependent variables must be established in all inactive control volumes. If the inactive region represents a stationary solid boundary as in the case, the velocity components in that region must be equal to zero, and if the region is regarded as isothermal boundary, the known temperature must be established in the inactive control volumes. Correspondingly, when a radiant intensity enters an inactive region, its magnitude becomes zero and it takes another boundary condition if it enters again to an active region. In a recent work, Lari and Gandjalikhan Nassab [16] studied coupled radiative and conductive heat transfer problems in complex geometries with inhomogeneous and anisotropic scattering participating media. In this work, the blocked-off method was used for simulating the complex geometry.

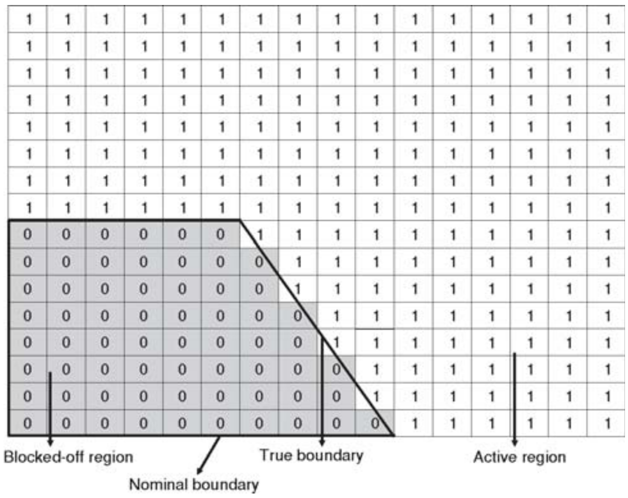

Figure 3. Blocked-off region in a regular grid

Code validation

Validation of convective heat transfer results

To verify the accuracy of computations in obtaining the heat transfer and flow characteristics of convection flow over BFS, the numerical implementation is validated by reproducing the results of two references. The results of re-attachment point in flow over a vertical BFS with expansion ratio of 2 and for different Re are compared with the experimental data, obtained by Armaly *et al*. [1], in fig. 4. As this figure shows, the re-attachment point moves toward the downstream side as the Re increases. However a good consistency is seen between the present numerical results with experiment.

In another test case for a convection flow over a BFS, the variation of Nu along the bottom wall is compared with the numerical results presented by Abu-Nada [6], in which the step was vertical to the stepped wall and the expansion ratio was considered to be equal to 2. The re-

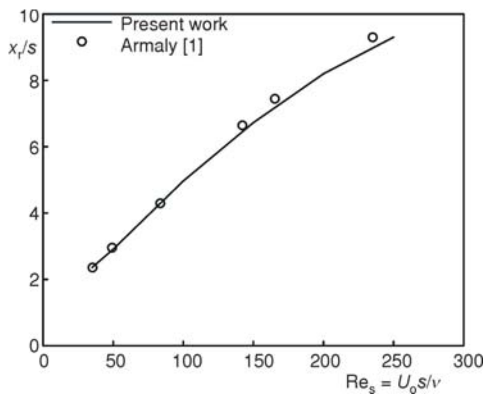

Figure 4. Variation of re-attachment length with Re; comparison with the results of Armaly [1]

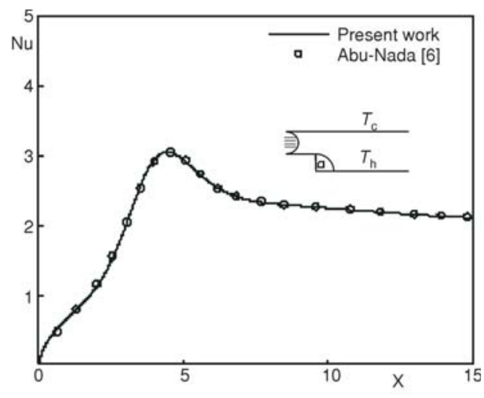

Figure 5. Distribution of convective Nu along the bottom wall; comparison with the results of Abu-Nada [6], Re = 400

sults are presented graphically in fig. 5 for the same condition as it is in ref. [6]. In this test case, the temperature of top wall was lower than the temperature of bottom wall and the temperature and velocity profile at the inlet section was assumed to be fully developed. The variation of Nu shows that the convection coefficient increases after the step up to the re-attachment point in which the maximum value of Nu takes place and then Nu decreases and approaches to a fixed value far from the step. However, fig. 5 shows a good consistency between the present numerical results with those reported by Abu-Nada [6]. It should be mentioned that as the radiating effect of the gas flow is neglected in that study, the gas flow is considered non-radiating in the computation of fig. 5.

Validation of combined conductive-radiative heat transfer results

Consider combined conductive-radiative heat transfer in a square enclosure of length L with optical thickness τ in either of direction, containing an absorbing, emitting and scattering medium. This problem was solved numerically in a study by Mahapatra *et al.* [17]. The boundary conditions are treated as hot wall on the left side and cold walls on the other sides such that all walls are black. Variation of mid-plane temperature is plotted in fig. 6 and compared with those obtained by Mahapatra *et al*. [17]. As it is seen a good agreement is achieved.

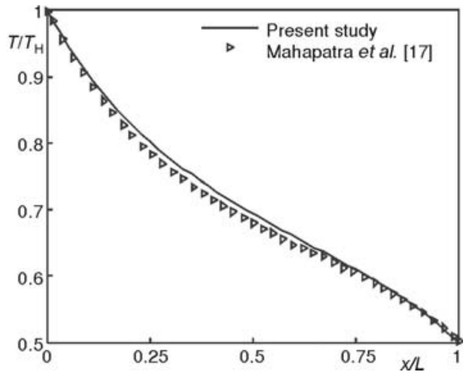

Figure 6. Variation of mid-plane temperature along the x-axis, RC = 10, ε = 1.0, τ = 1.0

Validation of the blocked-off method

To check performance and accuracy of the results obtained by the blocked-off technique, the blocked-off boundary treatment is applied to a semicircular enclosure with an inner circle as shown in fig. 7. This enclosure that contains an absorbing emitting and non-scattering medium was studied before by Byun *et al.* [18]. The medium is maintained at a constant temperature of 1000 K and the walls are assumed to be cold and black. The S_{10} approximation is used to calculate radiant intensity and the spatial grid of 100×50 is used in the x- and y-directions, respectively. The distribution of non-dimensional radiative heat flux along the bottom wall is shown in fig. 8 with comparison with the theoretical results by Byun *et al.* [18]. In that study, the

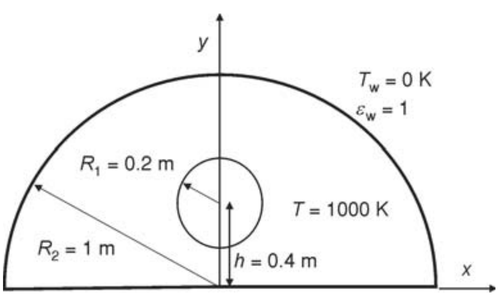

Figure 7. Schematic of semicircular enclosure

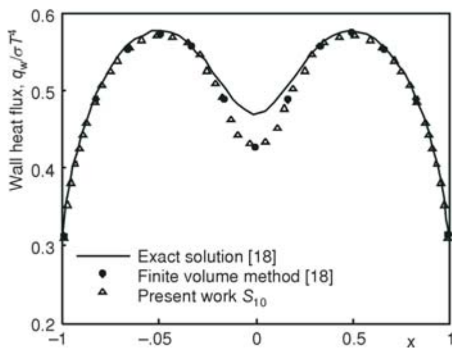

Figure 8. Radiative heat flux distribution on the bottom wall; comparison with the results in ref. [18]

blocked-off method along with the finite volume technique was employed in calculation of the radiant intensity. It can be seen that the non-dimensional radiative heat flux near the center is reduced and its minimum value occurs at the corners. This is due to cold semicircular wall and inner circle in which the intensity is influenced by the energy emitted from the intermediately far medium. However the solution obtained by the blocked-off treatment is shown to produce some error compared with exact solution as the Cartesian grid cannot exactly conform in shape to the inner circle and the semicircle.

Results and discussion

The present research results are presented for a forced convection laminar flow of a radiating gas over a 2-D inclined BFS in a horizontal duct at different *RC* and Re, while the value of Pr is kept constant at 0.71.

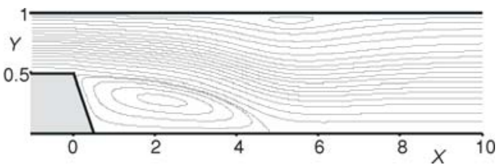

Figure 9. Stream lines contours, Re = 500, ϕ = 45°

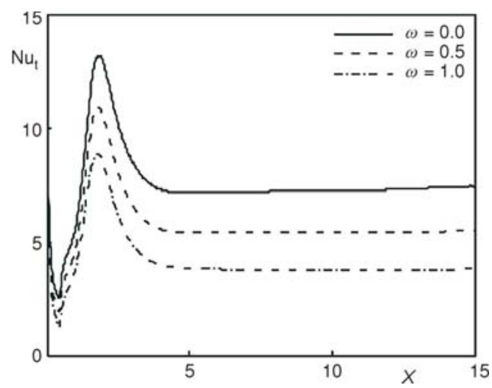

Figure 10. Effect of ω on the Nu*t* distribution along the bottom wall, *RC* = 100, τ = 0.005, Re = 100

First in order to show the flow pattern, the streamlines are plotted in fig. 9 for an inclined step with ϕ = 45° at Re = 500. The effect of inclined step on the flow is clearly seen from the curvatures of streamlines. Figure 9 shows that two re-circulation zones are encountered for Re = = 500 in the flow domain.

The primary re-circulation region occurs downstream the step adjacent the bottom wall, whereas the secondary re-circulation zone exists along the top wall. It should be noted that for small values of Re (say for Re < 350 for this test case), only the primary re-circulation zone appears.

For the convective flow with radiating heat transfer in the channel including a backward facing inclined step as shown in fig. 1, the distribution of Nu_t along the bottom wall is plotted in fig. 10. This figure shows that after the step location (X = 0), the value of Nu_t decreases sharply to its minimum value adjacent to the step corner, where the fluid is at rest. Then, the Nu_t increases, such that its maximum value occurs near the re-attachment point because of the flow vortices inside the re-circulated zone.

After the re-attachment point, the value of Nu_t decreases and then it approaches to a constant value as the distance continues to increase in the stream-wise direction.

Moreover, fig. 10 shows the effect of scattering albedo on the distribution of Nu_t along the bottom wall. The values of scattering albedo ω = 0.0 and ω = 1.0 correspond to non-scattering and pure scattering cases, respectively. As it is shown in fig. 10, the radiation effect which is enhanced at low value of scattering albedo, causes an increase in the value of local Nu_t which is significantly due to increase in Nu_r.

One of the main parameters in the combined conduction-radiation systems is the radiative-conductive (*RC*) parameter, which shows the relative importance of the radiation mechanism compared to its conduction counterpart. High value of *RC* parameter shows the radiation dominance in a thermal system. Variation of the convective and Nu_t along the bottom wall is plotted in fig. 11 with different values of the *RC* parameters. About the effect of *RC* parameter on the convective Nu_c, it can be seen from fig. 11(a) that Nu_c decreases by increasing in *RC*. This behavior is due to this fact that under the effective presence of radiation mechanism at high values of *RC*, the temperature field inside the flow domain becomes more uniform, consequently, the amount of temperature gradient inside the flow domain decreases that causes a decrease in the value of local Nu_c. It is worth mentioning that in the case of $RC = 0$, in which the maximum local Nu_c exists along the bottom wall, the radiative mechanism doesn't have any role in the heat transfer process. On the other hand, fig. 11(b) shows that the local Nu_t increases by increasing in *RC* which is due to increase in radiative part of Nu and the main Nu_t.

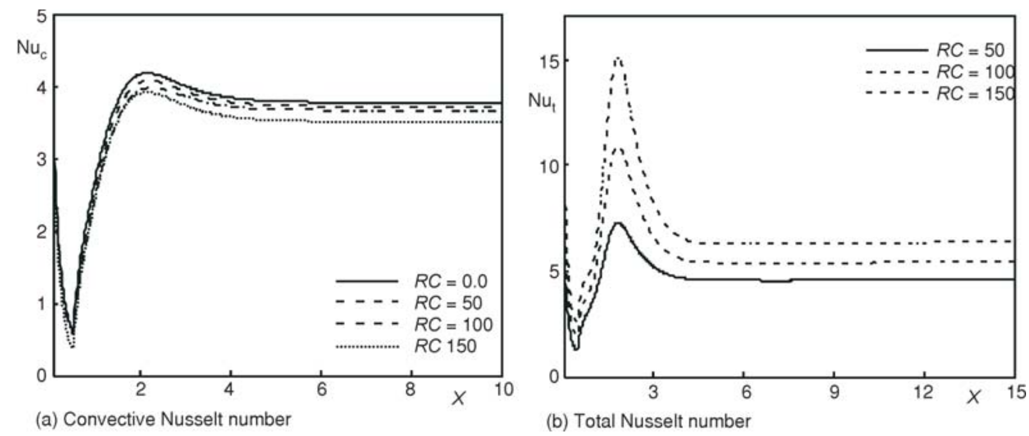

Figure 11. Effect of *RC* on the Nu distribution along the bottom wall, ω = 0.5, τ = 0.005, Re = 100

The optical thickness of a participating medium is a well-known radiation property that affects the temperature distribution. A higher value of τ, means that the medium's ability to absorb and emit radiant energy is greater. To study the effect of optical thickness on thermal behavior of the convective flow, fig. 12 shows the bulk mean temperature distribution along the duct at different value of τ. The case of transparent medium (corresponds to $\tau = 0$) is also presented in fig. 12 to compare the effects of radiation heat transfer. From this comparison, we can easily understand that the thermal development is augmented by radiation effect. It should be mentioned that in the computations related to the case of transparent medium with $\tau = 0$, the surface radiations from boundary walls are also omitted in the numerical procedure.

For the case of τ= 0.005 compared to τ = = 0.01, the bulk mean temperature increases from inlet to outlet. It is evident from fig. 12 that the bulk temperature increases more rapidly with an increase in optical thickness. As

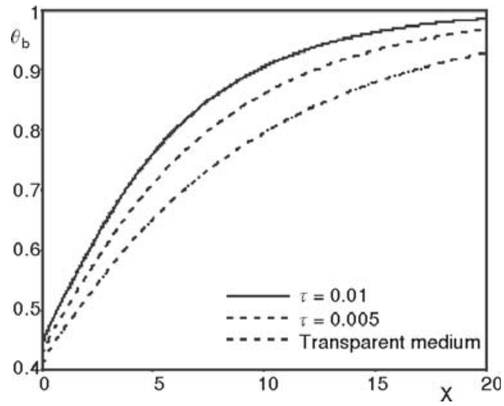

Figure 12. Effect of optical thickness on the bulk temperature distribution, Re = 200, *RC* = 100, ω = 0.5

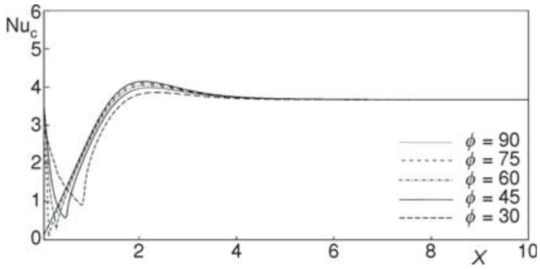

Figure 13. Effect of inclination angle on the Nu distribution along the bottom wall, RC = 100, ω = 0.5, τ = 0.005

expected, the fluid participates in the radiation transfer process by absorbing more energy radiated from the wall and emitting more energy to the medium at higher optical thickness values. Hence, the medium approaches the wall temperature at a much shorter distance from the entrance at higher optical thickness values.

As the present study focuses on the analysis of convective flow over an inclined step, to study the effect of step inclination angle on thermal behavior of the system, fig. 13 shows the distribution of local Nu_c along the bottom wall, at different values of ϕ.

It can be seen that the amount of maximum Nusselt number decreases by decreasing the step inclination angle which is due to shortening the length of re-circulated region and also decrease in the rate of flow vortices in the separated domain. In addition, it can be seen that by increasing the step inclination angle, the re-attachment point where the maximum Nu occurs, moves toward the downstream side.

Conclusions

The interaction between thermal radiation and forced convection in a laminar radiating gas flow over a 2-D backward facing inclined step in a duct has been studied in this paper. The set of governing equations including the conservation of mass, momentum and energy is solved numerically by the CFD technique. Since, the 2-D Cartesian co-ordinate system is used to solve the governing equations, the flow over inclined surface is simulated by considering the blocked-off region in regular grid. For calculating the radiative term in the energy equation, the RTE is solved by DOM to obtain the distribution of radiant intensity inside the radiating medium.

The effects of RC parameter, scattering albedo and optical thickness on the Nusselt number distribution along the bottom wall were presented. It was revealed that, these parameters have a great influence on the Nu distribution along the duct walls. It was shown that by increasing in RC the Nu_c decreases along the channel whereas the Nu_t increases which shows that the effect of Nu_r is greater than that of Nu_c on the Nu_t in the case of radiation dominant problem. In addition it was found that by decreasing in scattering albedo and increasing in optical thickness, the bulk temperature increases more and the development of temperature profile occurs rapidly at a much shorter distance.

Therefore, for having more accurate and reliable results in the analysis, the gas flow must be considered as a radiating medium and all of the heat transfer mechanisms including convection, conduction and radiation, must be taken into account. Such that in some cases in which radiation heat transfer takes an important role, neglecting this mechanism leads to large errors in the results.

Nomenclature

A_x,A_y – areas of control volume faces normal to the x- and y-directions, respectively, [m^2]
Be – Bejan number
c_p – specific heat, [$Jkg^{-1}K^{-1}$]
D_h – hydraulic diameter
ER – expansion ratio (= H/h)
I – radiation intensity [Wm^{-2}]
I^* – dimensionless radiation intensity
k – thermal conductivity, [$Wm^{-1}K^{-1}$]

Nu – Nusselt number
Nu_c – convective Nusselt number, [–]
Nu_r – radiative Nusselt number, [–]
Nu_t – total Nusselt number
$\vec{n}_w$ – outward unit vector normal to the surface
P – dimensionless pressure
p – pressure, [$kgm^{-1}s^{-2}$]
Pe – Peclet number, [–]
Pr – Prandtl number, [–]
$\vec{q}_r$ – radiative heat flux vector, [Wm^{-2}]
q_c – convective heat flux, [Wm^{-2}]
q_t – total heat flux, [Wm^{-2}]
q^* – dimensionless heat flux
Re – Reynolds number, [–]
RC – radiation-conduction parameter
$\vec{r}$ – position vector, [m]
S – radiation source function, [Wm^{-2}]
S^* – dimensionless radiation source function
$\vec{s}$ – geometric path vector
T – temperature, [K]
T_b – bulk temperature, [K]
u, v – velocity component in x- and y-direction, respectively, [ms^{-1}]
U, V – dimensionless velocity component in x- and y-direction, respectively
U_o – average velocity of the incoming flow at the inlet section, [ms^{-1}]
w_i – quadrature weight associated within any direction $\vec{s}$
x, y – horizontal and vertical distance, respectively, [m]
X, Y – dimensionless horizontal and vertical co-ordinate, respectively
x_1, x_2 – beginning and end of the secondary re-circulation bubble, [m]
x_r – re-attachment length, [m]

Greek symbols

α – thermal diffusivity, [m^2s^{-1}]
Θ – dimensionless temperature
Θ_b – dimensionless bulk temperature
θ_1, θ_2 – dimensionless temperature parameters (= 4 , 1.25), respectively
μ – dynamic viscosity, [Nsm^{-2}]
ρ – density, [kgm^{-3}]
σ – Stefan Boltsman's constant (= $5.67\cdot10^{-8}$), [$Wm^{-2}K^{-4}$]
τ – optical thickness
ω – scattering albedo

Subscripts

c – convective
in – inlet section
r – radiative
t – total
w – wall

References

[1] Armaly, B. F., *et al*., Experimental and Theoretical Investigation of Backward-Facing Step Flow, *Journal of Fluid Mechanics, 127* (1983), February, pp. 473-496
[2] Armaly, B. F., *et al*., Measurements in Three-Dimensional Separated Flow, *International Journal of Heat and Mass Transfer, 46* (2003), 19, pp. 3573-3582
[3] Erturk, E., Numerical Solutions of 2-D Steady Incompressible Flow over a Backward-Acing Step, Part I: High Reynolds Number Solutions, *Computers & Fluids, 37* (2008), 6, pp. 633-655
[4] Abu-Nada, E., Numerical Prediction of Entropy Generation in Separated Flows, *Entropy, 7* (2005), 4, pp. 234-252
[5] Abu-Nada, E., Entropy Generation Due to Heat and Fluid Flow in Backward Facing Step Flow with Various Expansion Ratios, *International Journal of Exergy, 3* (2006), 4, pp. 419-435
[6] Abu-Nada, E., Investigation of Entropy Generation over a Backward Facing Step under Bleeding Conditions, *Energy Conversion and Management, 49* (2008), 11, pp. 3237-3242
[7] Abu-Mulaweh, H. I., A Review of Research on Laminar Mixed Convection Flow over Backward- and Forward-Facing Steps, *International Journal of Thermal Sciences, 42* (2003), 9, pp. 897-909
[8] Gandjalikhan Nassab, S. A., *et al.*., Turbulent Forced Convection Flow Adjacent to Inclined Forward Step in a Duct, *International Journal of Thermal Sciences, 48* (2009), 7, pp. 1319-1326
[9] Viskanta, R., Overview of Convection and Radiation in High Temperature, *International Journal of Engineering Science, 36* (1998), 12-14, 10, pp. 1677-1699
[10] Azad, F. H., Modest, M. F., Combined Radiation and Convection in Absorbing Emitting and Anisotropically Scattering Gas-Particulate Flow, *International Journal of Heat Transfer, 24* (1981), 10, pp. 1681-1698
[11] Bouali, H., Mezrhab, A., Combined Radiative and Convective Heat Transfer in a Divided Channel, *International Journal of Numerical Mathematics, 16* (2006), 1, pp. 84-106
[12] Barhaghi, D. G., Davidson, L., Large-Eddy Simulation of Mixed Convection-Radiation Heat Transfer in a Vertical Channel, *International Journal of Heat and Mass Transfer, 52* (2009), 17, pp. 3918-3928

[13] Modest, M. F., *Radiative Heat Transfer*, McGraw-Hill, New York, USA, 2003
[14] Keshtkar, M. M., Gandjalikhan Nassab, S. A., Theoretical Analysis of Porous Radiant Burners under 2-D Radiation Field Using Discrete Ordinates Method, *Journal of Quantitative Spectroscopy & Radiative Transfer, 110* (2009), 17, pp. 1894-1907
[15] Patankar, S. V., Spalding, D. B., A Calculation Procedure for Heat, Mass and Momentum Transfer in Three-Dimensional Parabolic Flows, *International Journal of Heat and Mass Transfer, 15* (1972), 15, pp. 1787-1806
[16] Lari, K., Gandjalikhan Nassab, S. A., Modeling of the Conjugate Radiation and Conduction Problem in a 3-D Complex Multi-Burner Furnace, *Thermal Science*, *16* (2012), 4, pp. 1187-1200
[17] Mahapatra, S. K., *et al*., Analysis of Combined Conduction and Radiation Heat Transfer in Presence of Participating Medium by the Development of Hybrid Method, *Journal of Quantitative Spectroscopy & Radiative Transfer, 102* (2006), 2, pp. 277-292
[18] Young, B. D., *et al*., Investigation of Radiative Heat Transfer in Complex Geometries Using Blocked-Off, Multiblock and Embedded Boundary Treatment, *Numerical Heat Transfer Part A, 43* (2003), 8, pp. 807-825

Paper submitted: January 12, 2011
Paper revised: October 22, 2011
Paper accepted: October 26 2011